RHIC/RF-28

RHIC Project

BROOKHAVEN NATIONAL LABORATORY

RHIC/RF Technical Note No. 28

POWER AMPLIFIER FOR RHIC 26.7 MHz ACCELERATING CAVITY

S. Kwiatkowski, J. Brodowski, J. Greco, W. Pirkl, J. Rose

June 1995

POWER AMPLIFIER FOR RHIC 26.7 MHz ACCELERATING CAVITY.

S.Kwiatkowski, J. Brodowski, J.Greco, W.Pirkl, J.Rose

1. SUMMARY

This paper describes the 150kW 26.7MHz rf power amplifier which will power the accelerating cavities in the RHIC BNL synchrotron rings.

2. INTRODUCTION

The rf power amplifiers for 26.7MHz RHIC accelerating system have to be equipped with the closed loop fast feedback system for cavities voltage stabilization. System performance dictates a short signal delay in the feedback loop. For this reason, and in order to avoid the oscillations of the PA at the "transmission line" resonances final stage should be located in the machine enclosure and tightly coupled electrically and mechanically to the rf cavities. Additionally, since the amplifiers are subject to machine induced radioactivity components must resist radioactive damage. 4CW150000E EIMAC tetrode operating in the grounded cathode configuration will be used in the PA stage. Inductive coupling of the PA unit into the accelerating cavity has been chosen. The cross-section of the PA-cavity system is shown in Figure 1, and the electrical schematic of the rf power amplifier in Figure 2.

3. ANODE NETWORK DESIGN.

The optimum gap to anode voltage transformation ratio ($N=U_{g1}/U_{a1}$) for the maximum accelerating voltage (U_{g1}=400kV), and the available d.c. power supply (U_{aomax}=18kV d.c.) is about 25. The nominal anode voltage swing will be then 16kV ($U_{a1}=U_{g1}/N$).

3a. Power requirements.

The most demanding steady state conditions for the power amplifier unit will exist for the upgrade ring with the proton beam. Let us find out first the power requirements for this case for three characteristic points during the voltage ramp. The U_{g1} and $\sin\phi_s$ values over the ring cycle for proton beam are shown in Fig.3A and Fig.3B.

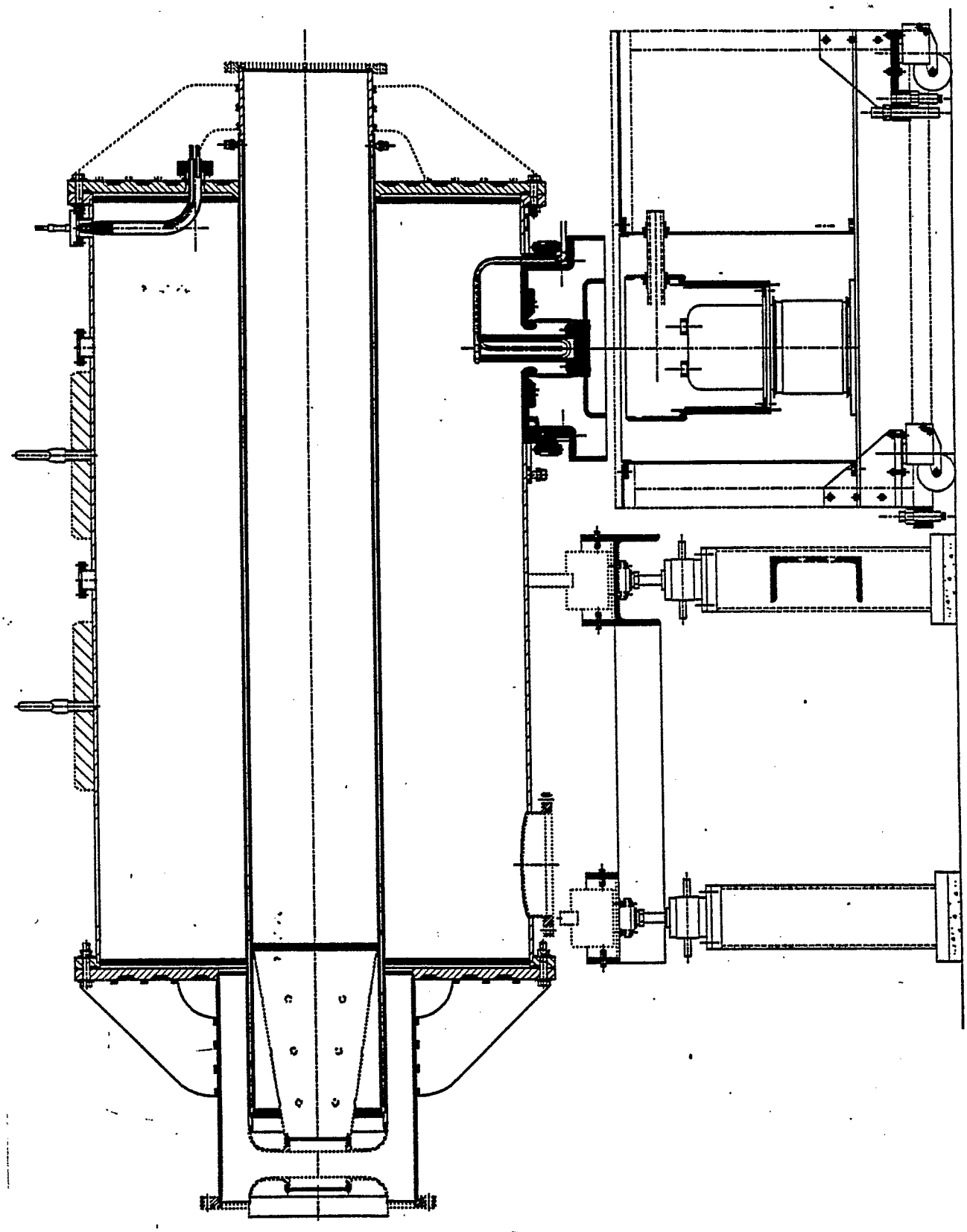

Figure 1

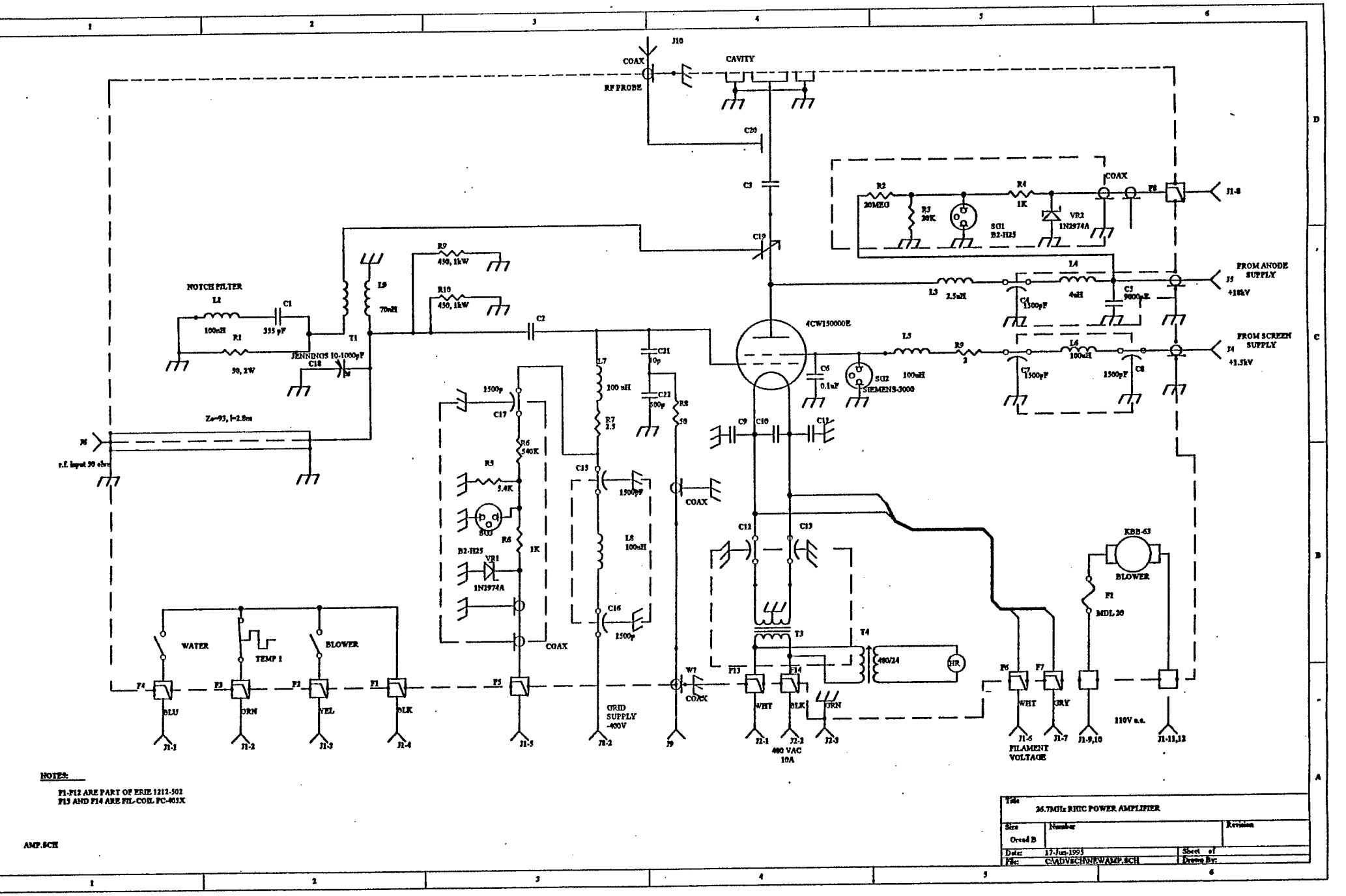
COAX
RF PROBE
J10
CAVITY
C20
C3
C19
R2
20MEG
R3
20K
R4
1K
SG1
B2-H25
VR2
1N2974A
COAX
F8
J1-8
L4
4uH
L3
2.5uH
C4
1500pF
C5
9000pF
FROM ANODE SUPPLY
J5
+18kV
L5
100uH
R9
2
C6
0.1uF
SG2
SIEMENS-3000
L6
100uH
C7
1500pF
C8
1500pF
FROM SCREEN SUPPLY
J4
+1.5kV
4CW150000E
NOTCH FILTER
L1
100nH
C1
355 pF
R1
50, 2W
T1
JENNINGS 10-1000pF
C18
L9
70nH
R9
450, 1kW
R10
450, 1kW
C2
L7
100 uH
R7
2.5
C21
10p
C22
500p
R8
50
C9
C10
C11
Zo=93, l=2.8m
J6
r.f. input 50 ohm
1500p
C17
R6
540K
R5
5.4K
SG3
R6
1K
B2-H25
VR1
1N2974A
C15
1500pF
L8
100uH
C16
1500p
COAX
COAX
COAX
C12
C13
T3
T4
480/24
HR
KBB-63
BLOWER
F1
MDL 20
WATER
TEMP 1
BLOWER
F4
F3
F2
F1
F5
W1
F13
F14
F6
F7
BLU
ORN
YEL
BLK
GRID SUPPLY -400V
WHT
BLK
GRN
WHT
GRY
J1-1
J1-2
J1-3
J1-4
J1-5
J8-2
J9
J2-1
J2-2
J2-3
480 VAC 10A
J1-6
J1-7
FILAMENT VOLTAGE
J1-9,10
110V a.c.
J1-11,12
NOTES:
F1-F12 ARE PART OF ERIE 1212-502
F13 AND F14 ARE FIL-COIL FC-405X
AMP.SCH
Title
26.7MHz RHIC POWER AMPLIFIER
Size
Orcad B
Number
Revision
Date: 17-Jun-1995
File: C:\ADVSCH\NEWAMP.SCH
Sheet of
Drawn By:

Figure 2

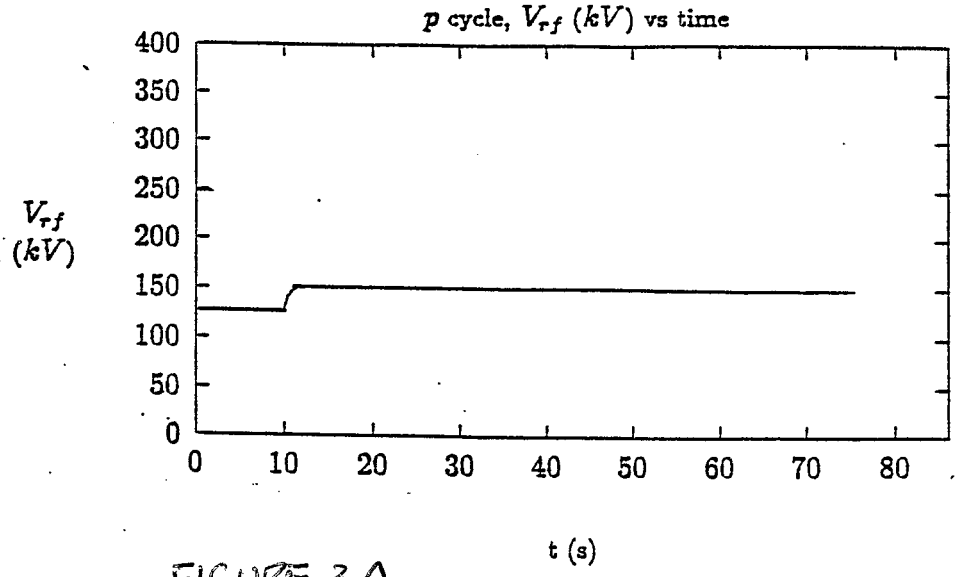

FIGURE 3A

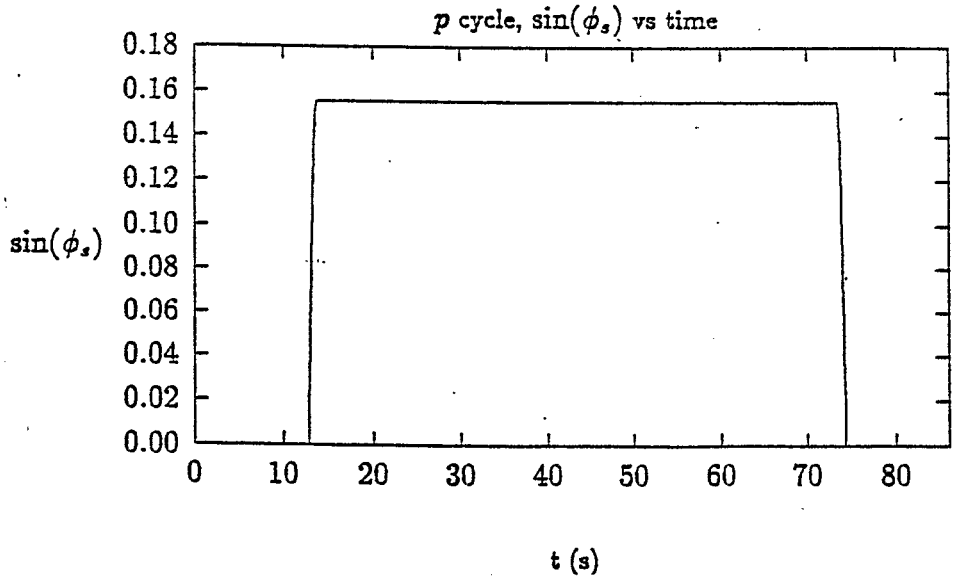

Figure 3B

The vector diagrams for currents and voltages for the three characteristic points of the ramp are shown in Fig.4A(injection), Fig.4B(acceleration) and Fig. 4C ("high voltage "period).
The power amplifier calculations have been done for each characteristic point of the cycle for two cases:

a. Amplifier detuned for the beam loading compensation.
b. Amplifier tuned ($f_{cav}=f_{rf}=h \bullet f_{rev}$)

The results are shown in Table 1.

Input data:

Cavity data (SUPERFISH results): R_{sh}=940kΩ, Q=15650, R/Q=60Ω
$N=U_{gl}/U_{al}$=25; U_{adc}=18kV; $U_{sd.c.}$=1.5kV; $U_{gd.c.}$= -380V; I_{a0}=1A; R_{in}=200Ω; $R_a=R_{sh}/N^2$=1.5kΩ

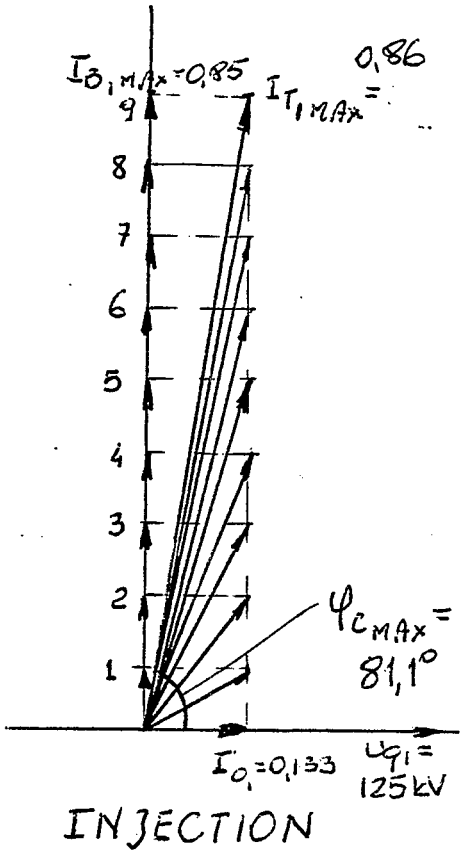

Figure 4A

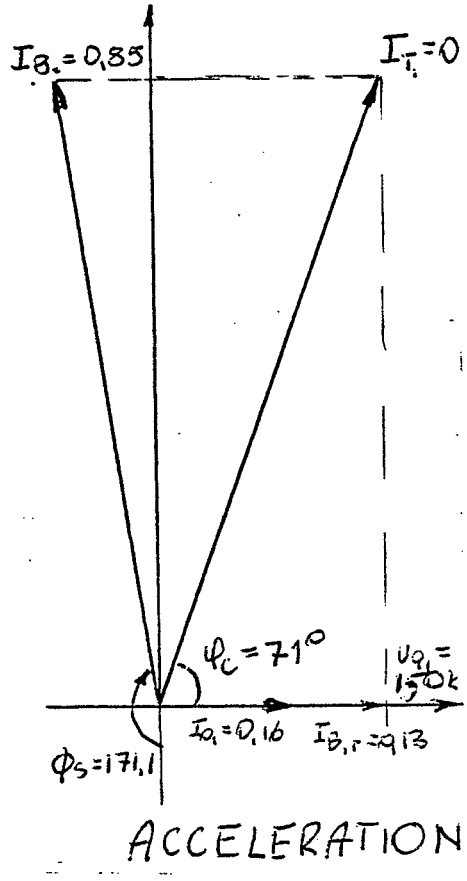

Figure 4B

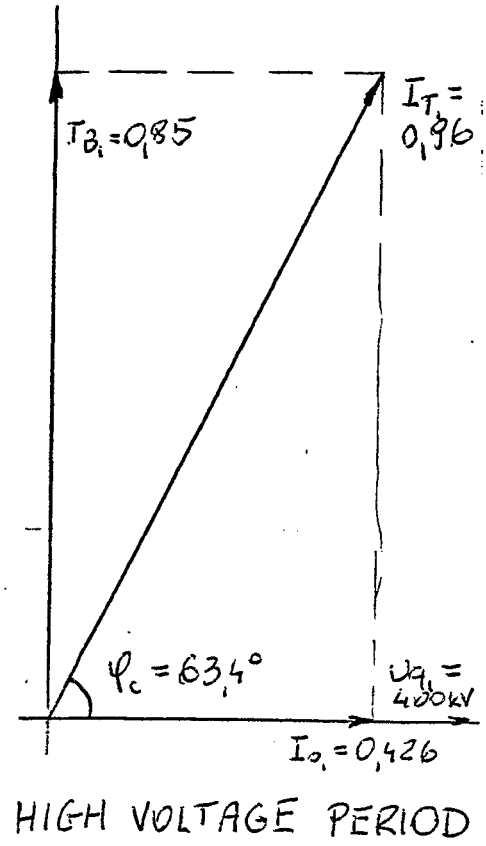

Figure 4C

	INJECTION		ACCELERATION		HIGH VOLTAGE	
Value	Cavity detuned for the beam loading compensation	Cavity tuned	Cavity detuned for the beam loading compensation	Cavity tuned	Cavity detuned for the beam loading compensation	Cavity tuned
U_{a1} [kV]	5	5	6	6	16	16
I_{a1} [A]	3.3	21.5	7.3	22.3	10.64	23.8
I_{adc} [A]	2.2	13.6	4.9	14.1	7.3	15
P_{a1} [kW]	8.3	8.3	21.9	21.9	85.1	85.1
$P_{ad.c.}$ [kW]	40.3	244.0	88.2	254	131.4	270
P_{a0} [kW]	32.0	235.7>P_{adm}	66.3	232>P_{adm}	46.3	184.9>P_{adm}
η_a [%]	20.6	3.4	24.8	8.6	64.8	31.5
U_{gr1} [V]	110	340	180	350	270	370
P_{inp} [W]	30	290	81	306	182	342

TABLE 1

where: U_{a1}-First harmonic component of the anode voltage. $U_{a1}=U_{g1}/N$
I_{a1}- First harmonic component of the anode current
$I_{ad.c.}$-D.c. component of the anode current
P_{a1}-Resistive power. $P_{a1}=0.5 \bullet I_{a1} \bullet U_{a1} \bullet \cos\phi_c = U_{g1}^2/2R_{sh}$
P_{adc}-D.c. power. $P_{adc}=U_{adc} \bullet I_{adc}$
P_{a0}- Power dissipated at the anode. $P_{a0}=P_{adc}-P_{a1}$
P_{adm}- Tube anode rating (for 4CW150000E tetrode P_{adm}=150kW)
η_a- Anode efficiency. $\eta_a=P_{a1}/P_{adc}$
U_{gr1}-First harmonic component of the grid voltage(from 4CW150000E characteristics)
P_{inp}-Drive power. $P_{inp} \approx U_{g1}^2/2R_{inp}$ ($R_{inp}=200\Omega$).

When the rf cavity is detuned for the beam loading compensation, the cavity impedance being no longer tuned at r.f. frequency excites the coupled bunch instabilities. The estimations of the growth rate of the CBM (Couple Bunch Modes) for the r.f. system with the fast feedback gain of 40dB over all ramp period has been done using CNN2 program (software developed in INS Laboratory in Novosibirsk, Russia), and the results are given below.

1. Gold - 57 bunches 1e9 particles per bunch	S_3=0.32
2. Gold -114 bunches 1e9 particles per bunch	S_3=0.85
3. Protons-57 bunches 1e11 particles per bunch	S_2=0.43
4. Protons-114 bunches 3e11 particles per bunch	S_2=13.7- too much.

The growth rate of the CBM for the high intensity protons beam is too large and it is impossible to correct this problem by tuning the power amplifier into the resonance (by means of feedforward system or additional feedback loop as it is done in Fermilab main ring) due to the anode power dissipation limit (active damper required).

The most demanding instantaneous requirements for the r.f. systems exists during transition crossing period (all ions except protons). During this procedure the phase of the rf drive changes instantaneously by 162°, thou the r.f. power source has to operate at the mismatched load during short period(less than 100 microsecond for 40 dB fast feedback gain). The analysis and the simulation of the 26.7 MHz system with the 40dB fast feedback gain and the 600ns delay in the feedback loop has been done and the results are given in Fig.5, 5A and 5B. Figure 5 showes the response of the system to the 162° fase jump in the case when there is no power limitation in the rf amplifier chain. In the Figure 5A driver amplifier is limited to 4kW (solid state driver amplifier is the element in the rf amplifier chain which limits the inststenous power capability of the system), and in Fig 5B limit is 1kW. In the first case the cavity voltage has been reestablished after 4us in the second case after 45us and in the third case after 90us. Beam dynamic analysis show that if during transition period the r.f. system is unable to maintain the correct value of the cavity voltage for the period smaller than ten times beam revolution period (10*13us), no degradation of the beam quality is expected

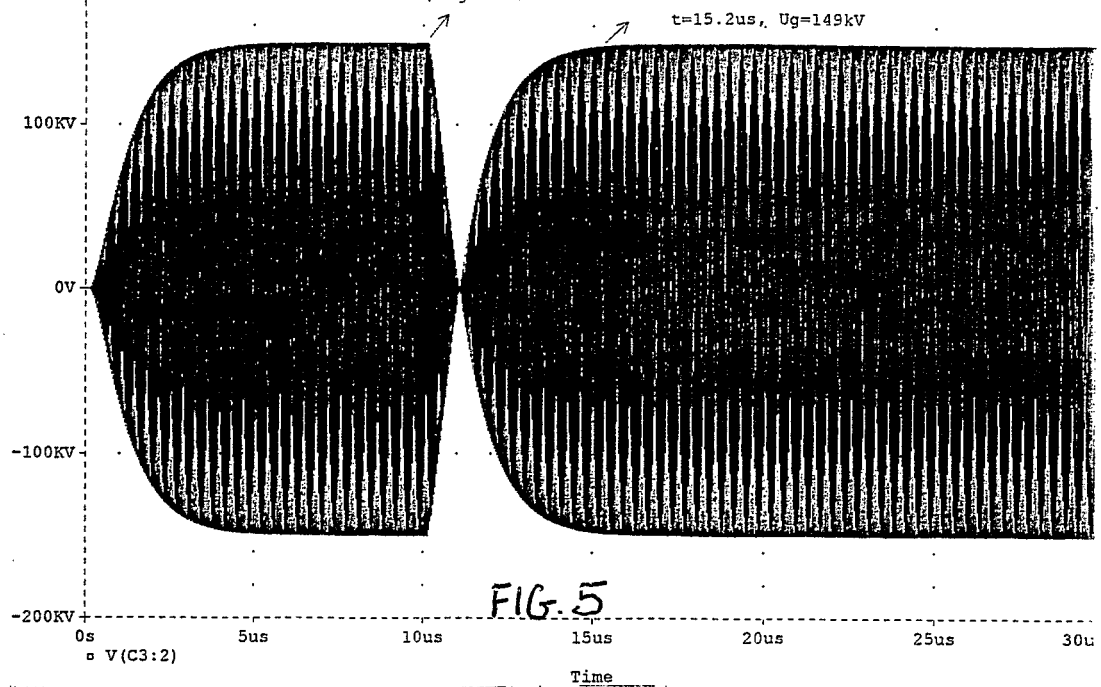

FIG. 5

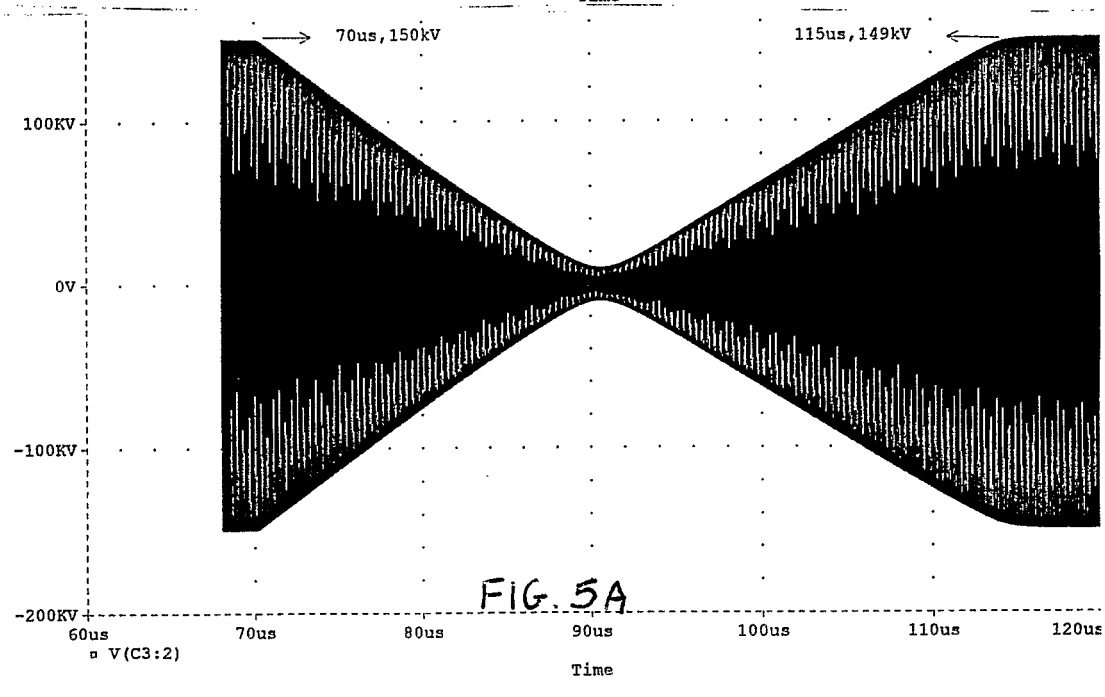

FIG. 5A

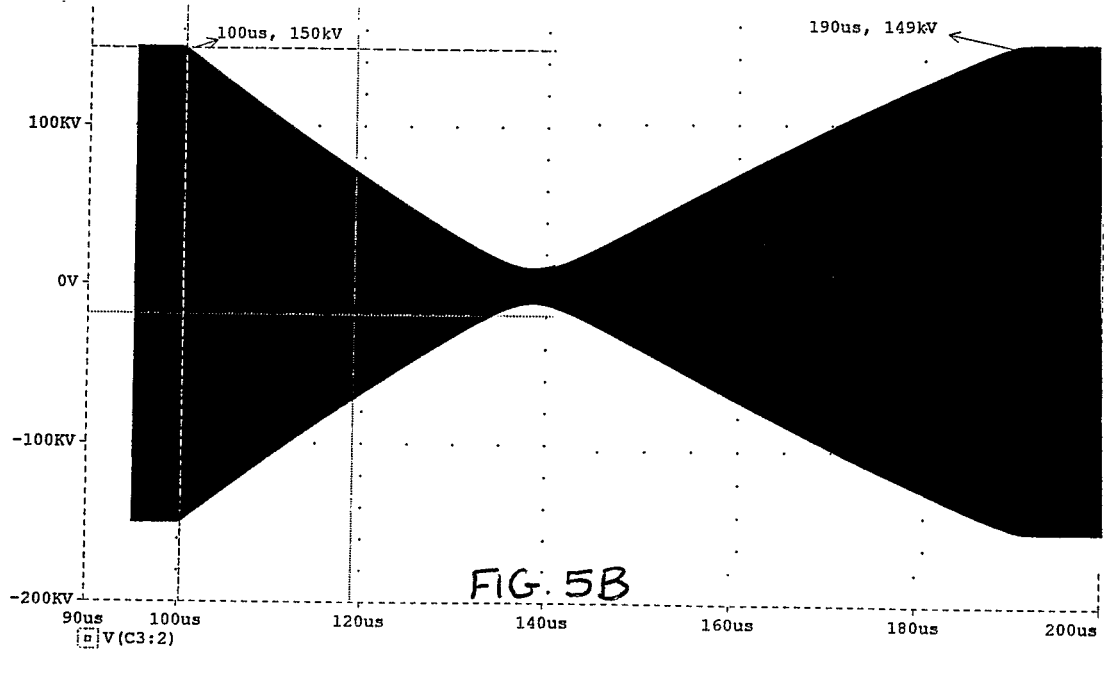

FIG. 5B

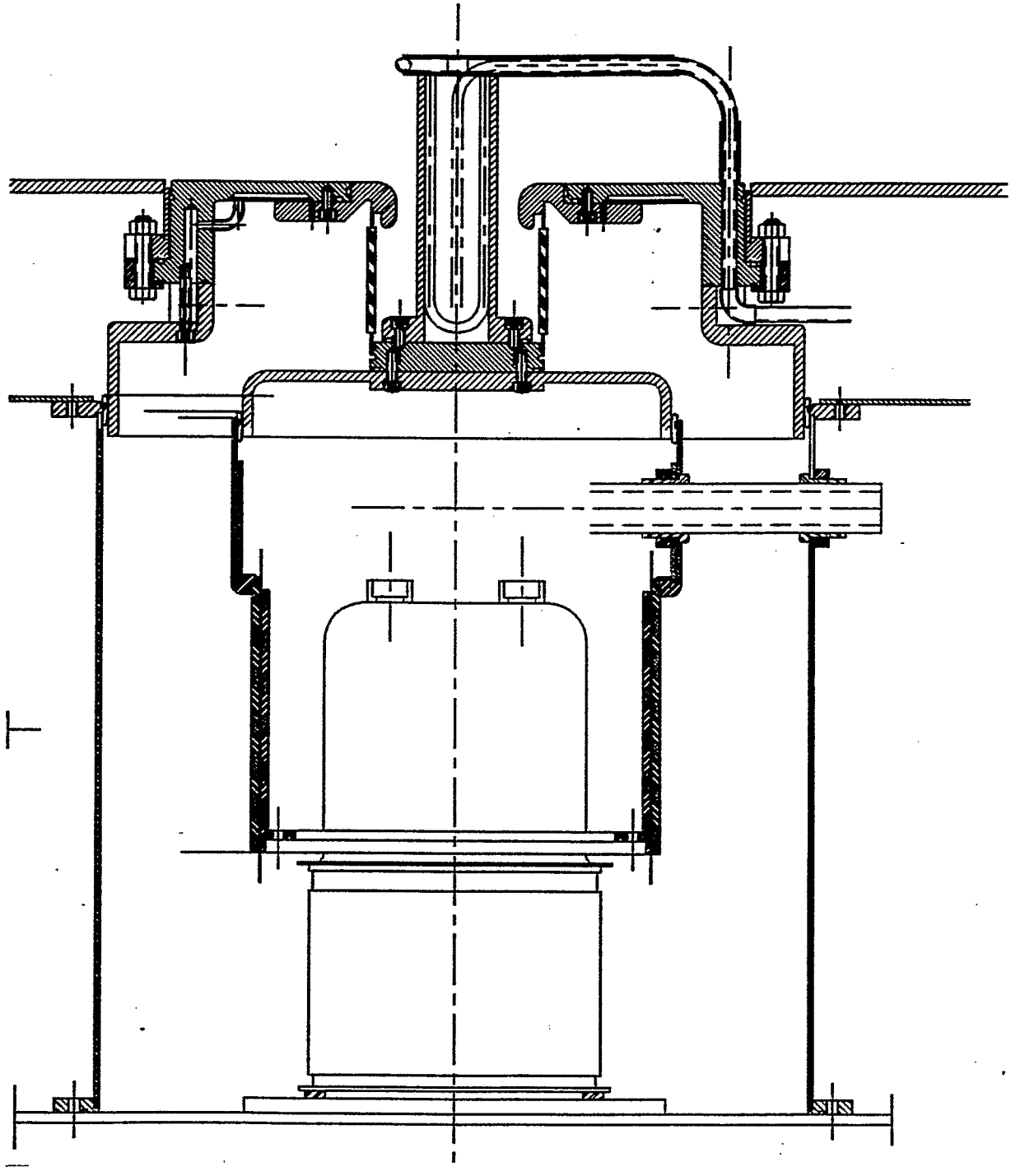

Figure 6

3b. Anode network calculation.

The cross-section of the power amplifier unit is shown in Fig.6. The basic parameters of the r.f. cavity-anode network structure have been calculated using 3-D final element MAFIA code. The results of the calculations are given in Table 2.

Frequency	F [MHz]	26.7
Gap Voltage	U_{gl} [kV]	400
Cavity Shunt Impedance	R_{sh} [kΩ]	940
Cavity Quality Factor	Q [-]	15670
R_{sh}/Q	R_{sh}/Q [Ω]	60
Stored Energy	W [J]	8
Maximum H-field	Hmax [A/m]	8900
Anode circuit resonance frequency	F [MHz]	37
Coupling loop self inductance	Ll [nH]	103
Mutual inductance	M [nH]	6
Power losses in the coupling loop(for Ug=400kV)	P_l [W]	985
Power losses in the anode network	Pa [W]	1200

Table 2

3b. Lumped constant anode-cavity network model

Based on the MAFIA calculations the simple lumped constant model has been created and is shown in Fig.7.

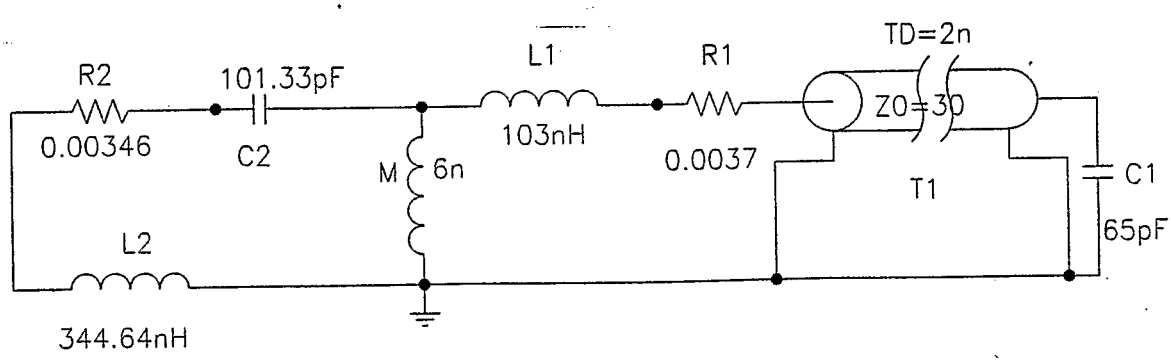

Figure 7

3c. Vacuum window design.

Two versions of the vacuum window for 26.7MHz accelerating system has been considered and fully analyzed (coaxial and planar windows). The results of the calculations for the windows made out of Alumina 97.3% are given in Table 3. All calculations have been done for 400kV accelerating gap voltage and gap-to anode voltage transformation ratio=25

Windows dimensions: coaxial L*D1*D2= 70*114.5*104.5[mm]
planar L*D1*D2= 20*280*70 [mm]

	coaxial	planar
Maximum tang. component of the E-field at the ceramic surface	2.7[kV/cm]	3.7[kV/cm]
Power losses for tgδ=0.0005	5.0[W]	80[W]
Average power density in ceramic	40[mW/cm^3]	70[mW/cm^3]
Peak power density in ceramic	100[mW/cm^3]	220[mW/cm^3]
Maximum temperature gradient across the ceramic	0.17 degC	1.5 degC

Table 3.

Coaxial window has been chosen as a front running design due to their better electrical performances. The electrostatic program SAM was used to find out the final geometry of the vacuum window. The tangential component of the E-field at the surface of the vacuum window is shown in Fig.8.

3.d Coupling loop.

The basic dimensions of the coupling loop have been determined based on MAFIA code results and are shown in Fig.9. The adjustment of the coupling between the PA and the accelerating cavity will be done by rotation of the coupling loop.

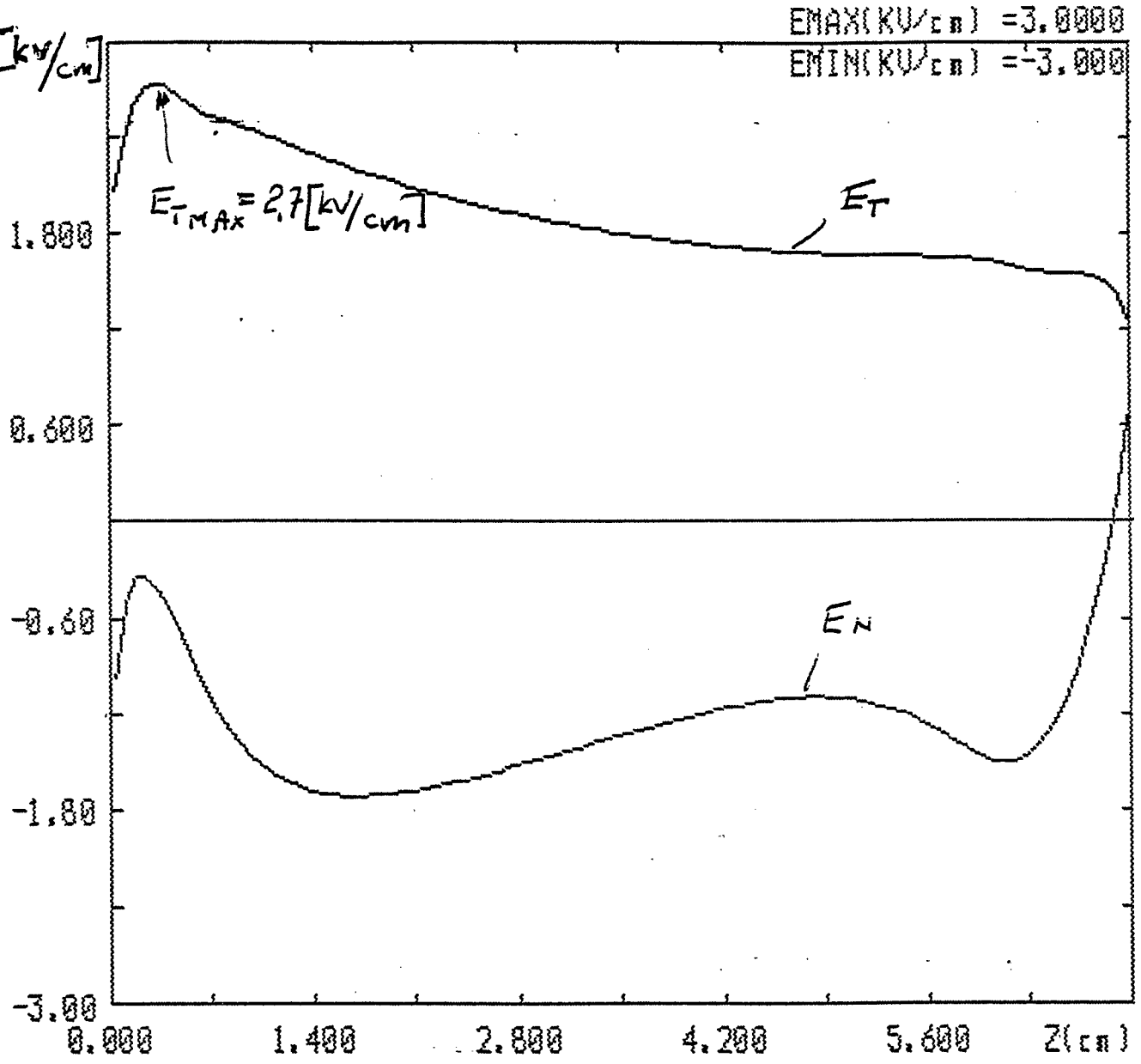


```
Display the normal and tangential components of field
M - near the metallic surface
D - near the dielectric surface
[M,D] :
```

Figure 8

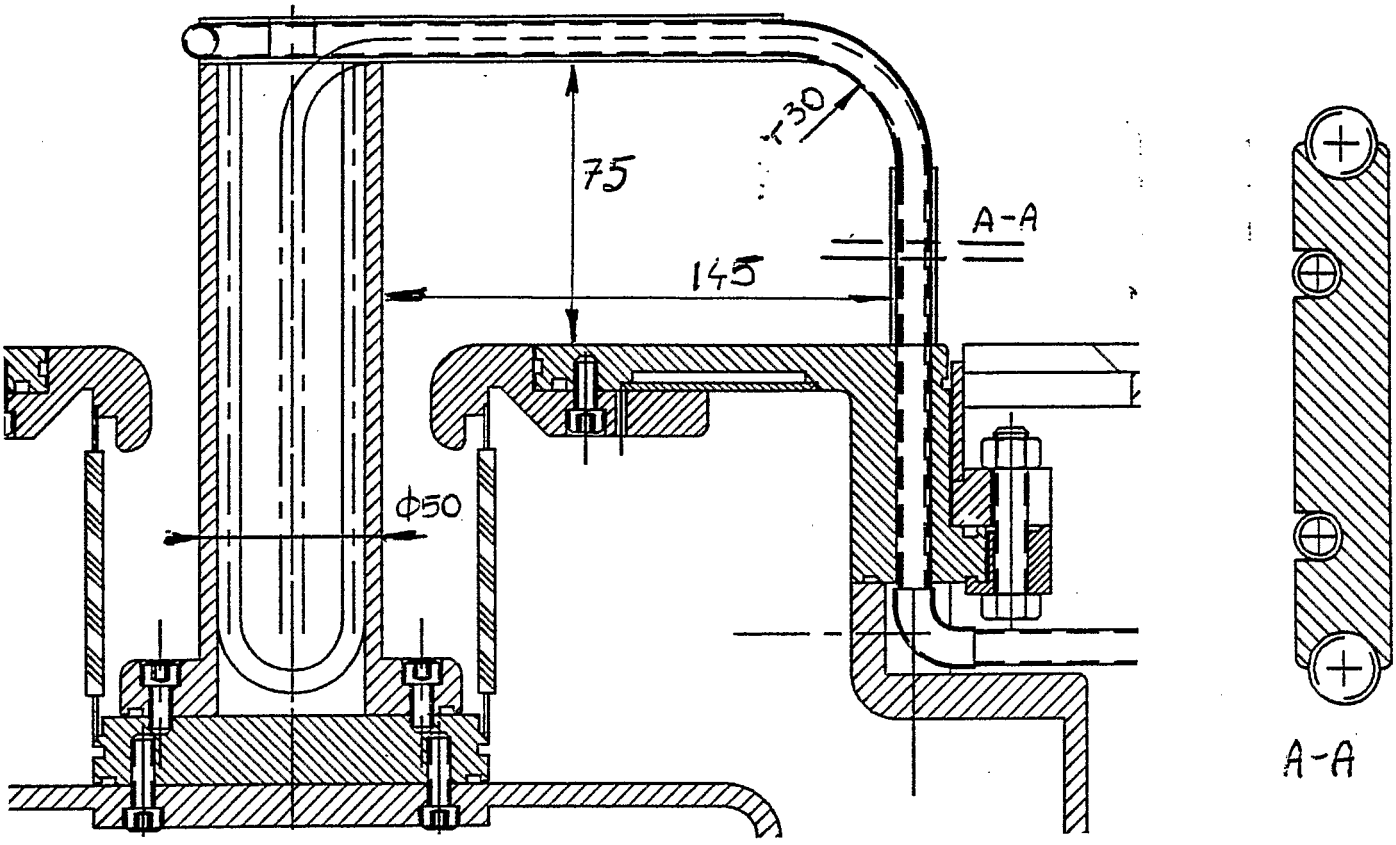

Figure 9.

4. POWER AMPLIFIER STABILITY ISSUE.

The schematic diagram of the typical tetrode amplifier is shown in Fig.10. Effective input capacitance and the resistance of the power amplifier in the neighborhood of the resonance frequency could be find out as follow:

$$C_{in}=C_{gk}+C_{gs}+C_{ag}(1+k\bullet\cos\varphi_a)$$
$$1/R_{in}=1/R_d - \omega\bullet C_{ag}\bullet k\bullet\sin\varphi_a$$

where: C_{gk}-grid to cathode capacitance
C_{gs}-grid to screen capacitance
C_{ag}-grid to anode capacitance
k-voltage amplification factor($k=U_{a1}/U_{g1}$)
φ_a-anode network detuning angle
R_d-grid load resistor

The PA unit could oscillate if the effective input resistance is negative. So in our case for C_{ag}=1[pF] and k<60 amplifier will be unconditionally stable in the neighbourhood of the operating frequency if the $R_d<100\Omega$.

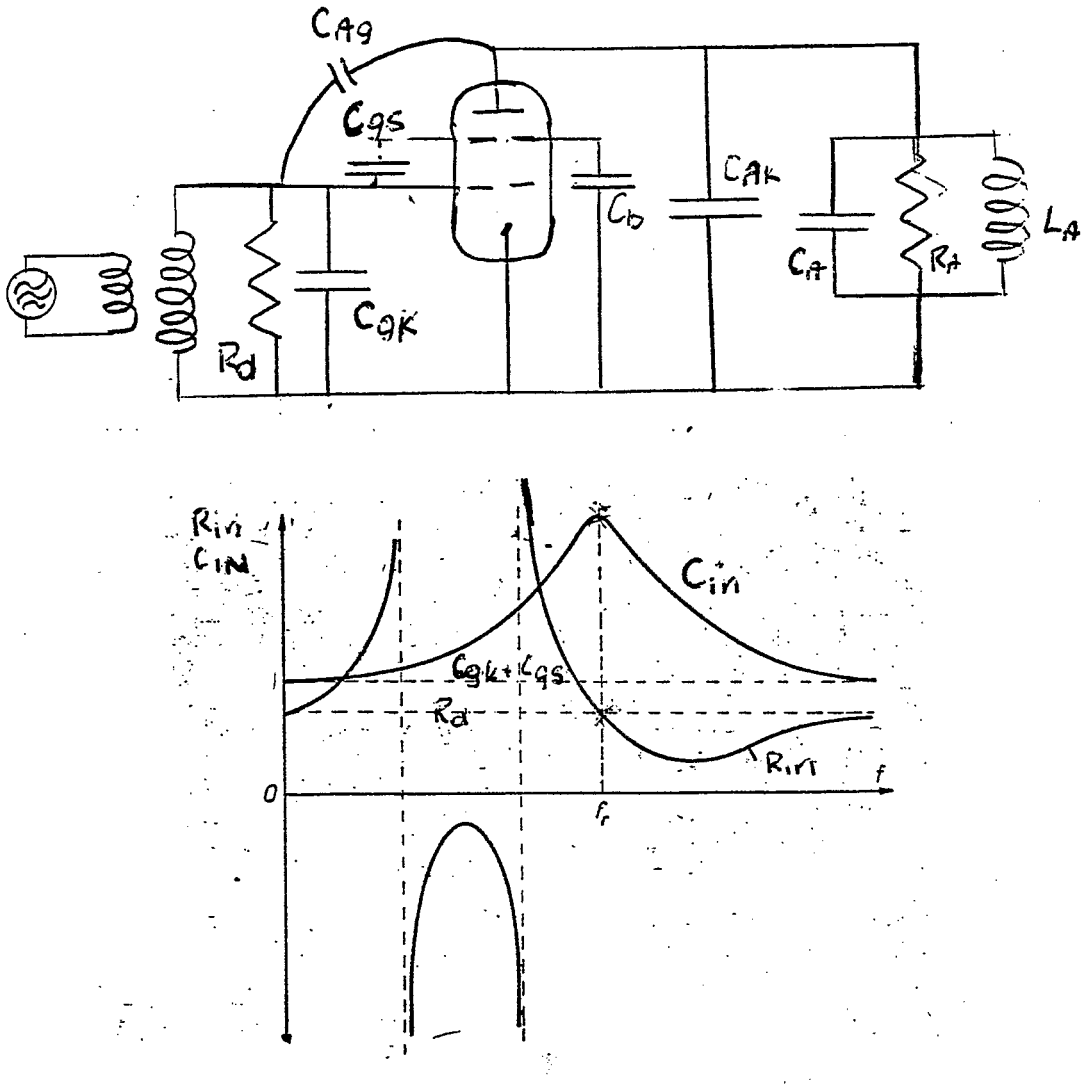

Figure 10

5. INPUT NETWORK.

The input network is shown in Fig.11. It is build as a simple parallel resonance circuit with the load resistance of 200Ω. Jennings 10-1000pF condenser is used to tune the input network in the resonance. 1kW solid state driver has 50Ω output impedance and the matching between 50Ω r.f. line and the 200Ω input impedance is done by use of λ/4 transformer made out of 93Ω RG-58 coaxial cable.

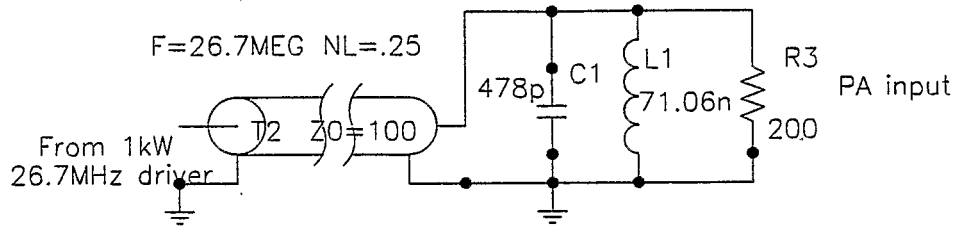

Figure 11.

6. NEUTRALIZATION CIRCUIT.

Since the input impedance of the PA unit has been chosen higher than 100Ω, the amplifier has to be equipped in the neutralization circuitry. Neutralization circuit is composed out of C19, T1, L1, C1 and R1(see Fig.2). C19 value has to be equal Cag_1 of the power tube(about 1.2pF for 4CW150000E tetrode). Transformer T1 is build out of semirigid 50Ω transmission line and works as a simple 1:1 ballun. Outer conductor of the 50Ω balun is used simultaneously as inductance of the input network. At the fundamental frequency the "grid side" of the inner conductor of the balun is grounded (C1 and L1 tuned into the resonance), when at other frequencies it is terminated into the 50Ω load(R1).

7. PSPICE MODEL

To investigate the behavior of the whole PA-cavity system the lumped constants model has been created and analyzed using PSPICE software. The lumped constant model is shown in Fig.12. The influance of neutralization circuitry on the performances of the system could be observed at the Figure.13, and the Figure 14. Both pictures show the tube input voltage in the function of the frequency in the neighbourhood of the operating frequency. In the first case the neutralization circuitry was not used and in the second case it was used and the neutralization capacitance was equal the tube feeedback capacity Cag. Here the transfer energy between the input and the output network of the power tube at the fundamental frequency has been completely stopped.

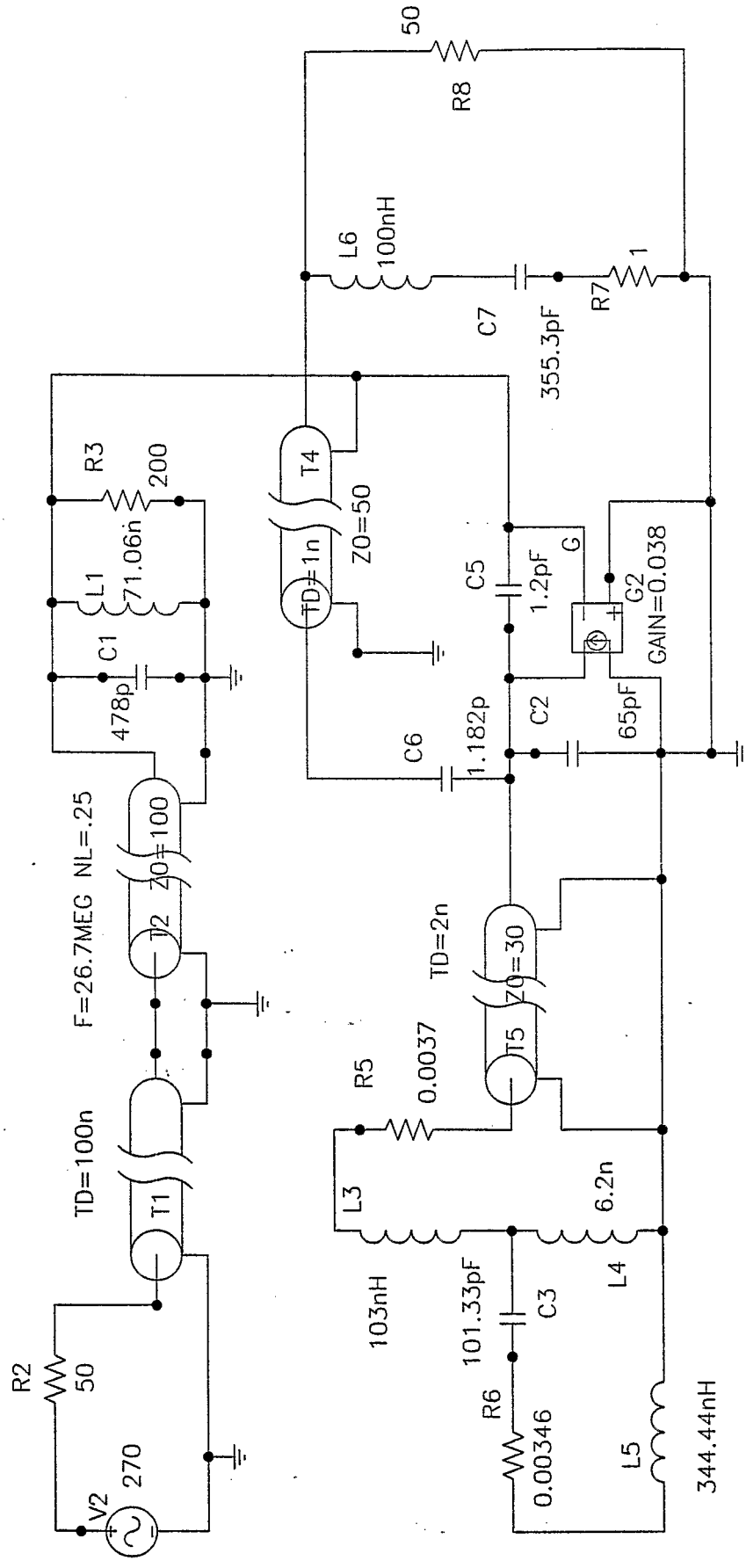
50
R8
L6
100nH
1
R7
C7
355.3pF
R3
200
T4
Z0=50
TD=1n
L1
71.06n
C5
1.2pF
G
G2
GAIN=0.038
C1
478p
C2
65pF
C6
1.182p
F=26.7MEG NL=.25
Z0=100
T2
TD=2n
Z0=30
T5
R5
0.0037
TD=100n
T1
L3
6.2n
103nH
101.33pF
C3
L4
R2
50
R6
0.00346
L5
344.44nH
V2
270

Figure 12

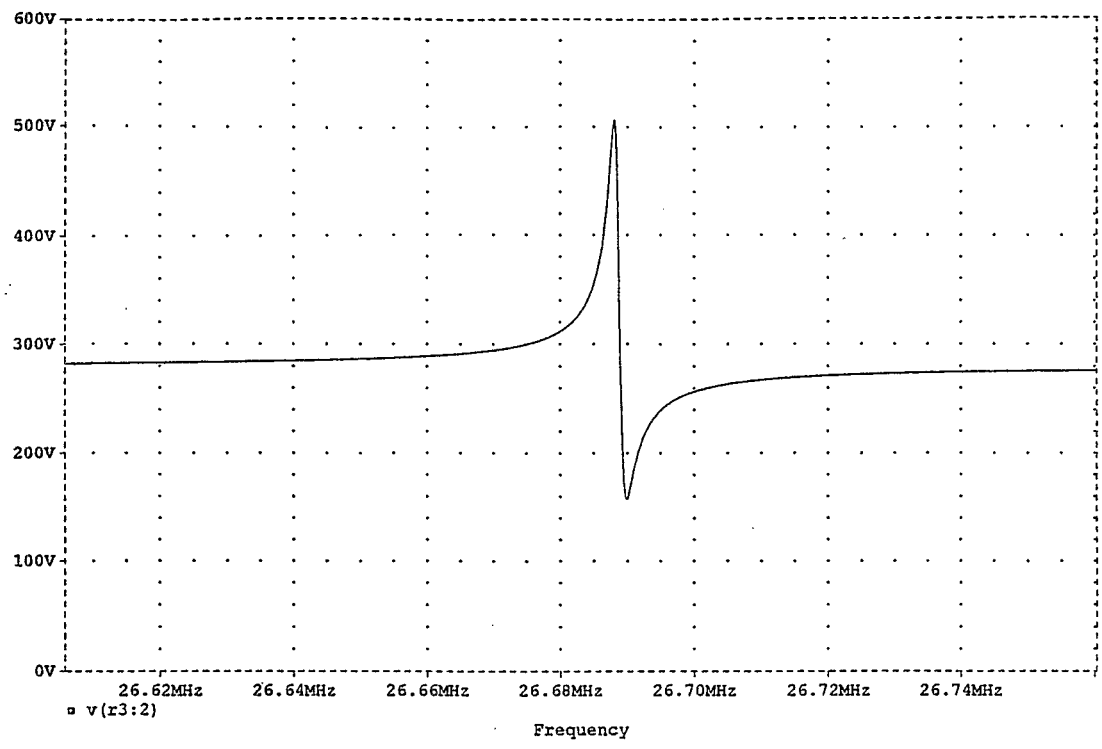

Figure 13

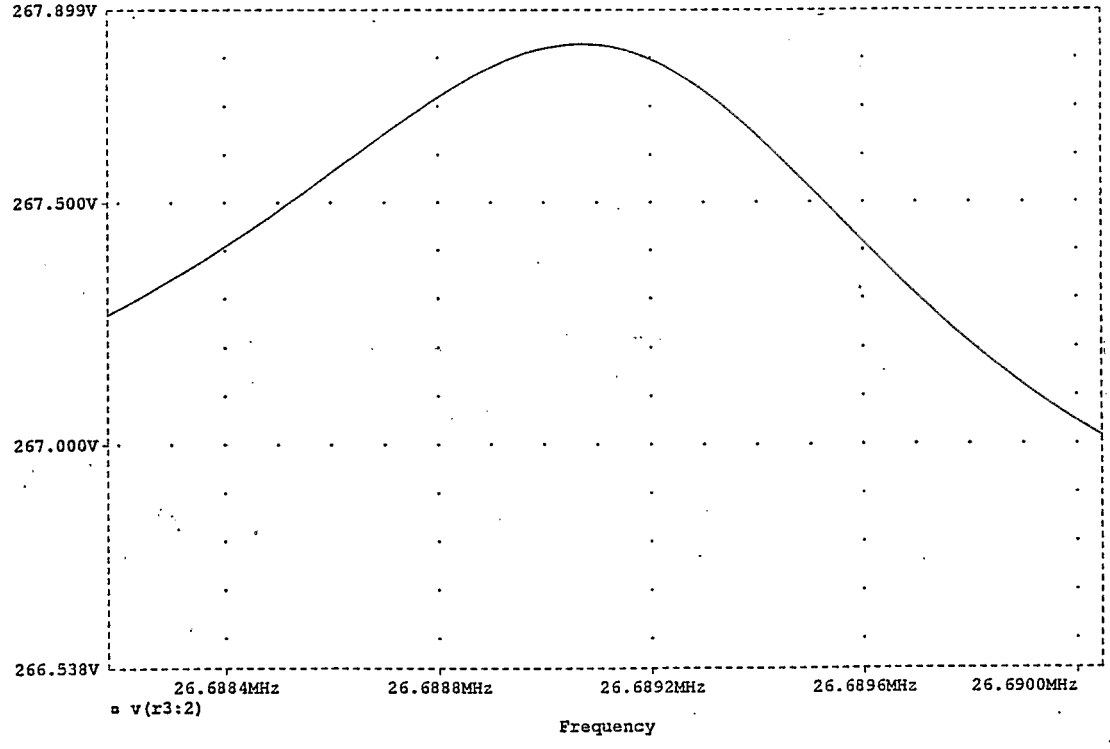

Figure 14

8. ANODE BLOCKING CIRCUIT.

The r.f. voltage at the input of the high voltage power supply could reach 14[kV](for 16[kV] anode voltage swing). The rf anode filter should attenuate the rf signal by at least 50dB. Schematic diagram of the filter is shown in Fig.14.

R.f choke data:

Coil length	28[cm]
Number of turns	15
Inductance	2.5[μH]
Mid-wire diameter	5.6[cm]
Length of wire	240[cm]
Distributed capacity	5.5[pF]
Self resonance frequency	43[MHz]
R.f. current in coil	38[A]
Power losses	50[W]

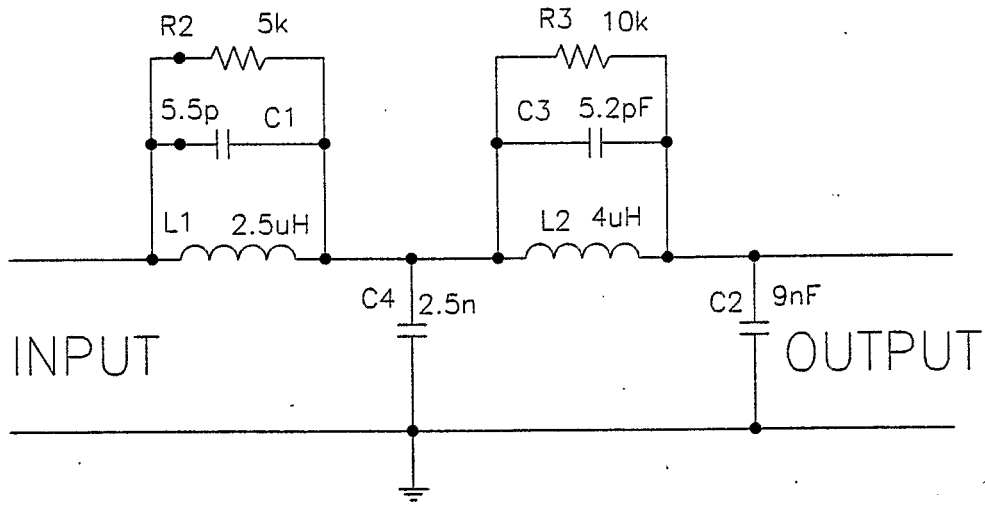

Figure 15.

"Spice" program was used to calculate the anode filter. The response of the filter is shown in Fig.16. Theoretical attenuation factor at 26.7MHz is 115[dB]. Maximum current in the first blocking capacitor is 30[A]. The test results of the prototype of the anode filter are shown in Fig.17.

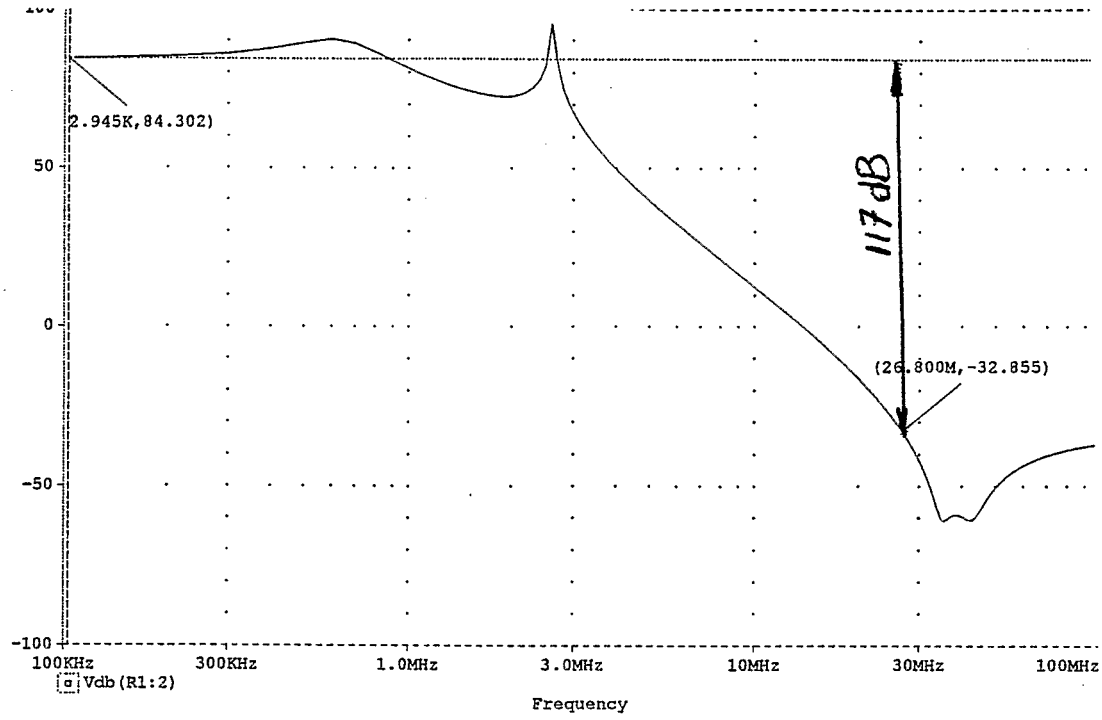

Figure 16

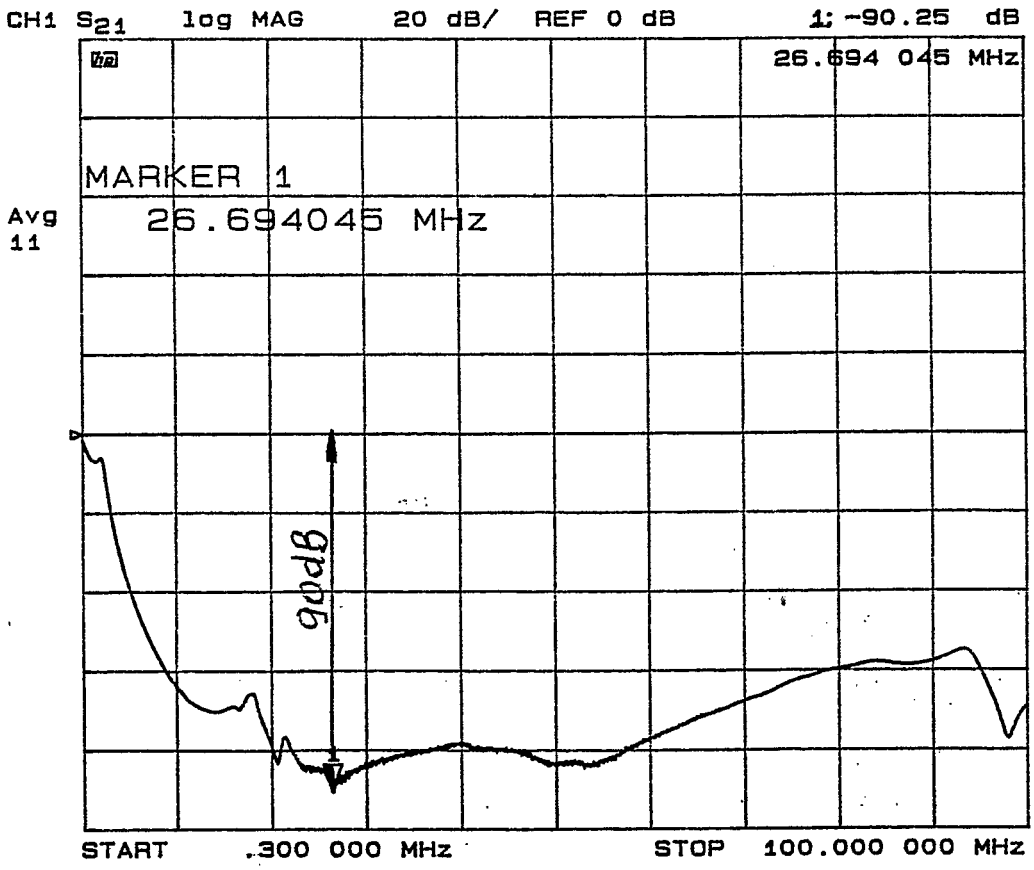

Figure 17

6. SCREEN BLOCKING CIRCUIT.

Sk-2011A tube socket that will be used in our amplifier has build-in 13[nF] screen blocking capacitance. The first self resonance frequency (series resonance) is at 16[MHz]. At 26.7[MHz] screen impedance is $1.5e^{j60}$(measured value). The screen blocking circuit is shown in Fig.2(elements C6, SG2, L5, R9, C7, L6, C8)